Partial Slip Effect on Heat and Mass Transfer of MHD Peristaltic Transport in a Porous Medium
(Kesan Gelincir Separa ke atas Pemindahan Haba dan Jisim bagi Aliran Peristalsis MHD di dalam Medium Berliang)

OBAID ULLAH MEHMOOD, NORZIEHA MUSTAPHA*, SHARIDAN SHAFIE & T. HAYAT

ABSTRACT

This research looks at the effects of partial slip on heat and mass transfer of peristaltic transport. The magnetohydrodynamic (MHD) flow of viscous fluid in a porous asymmetric channel has been considered. The exact solutions for the stream function, longitudinal pressure gradient, longitudinal velocity, shear stress, temperature and concentration fields are derived by adopting long wavelength and small Reynolds number approximations. The results showed that peristaltic pumping and trapping are reduced with increasing velocity slip parameter. Furthermore, temperature increases with increasing thermal slip parameter. Moreover, the concentration profile decreases with increasing porosity parameter, Schmidt number and concentration slip parameter. Comparisons with published results are found to be in good agreement.

Keywords: Heat and mass transfer; MHD peristaltic flow; partial slip; porous medium; pumping; trapping

ABSTRAK

Kajian ini membincangkan kesan gelincir separa ke atas pemindahan haba dan jisim bagi aliran peristalsis. Aliran yang mempunyai hidrodinamik magnet (MHD) di dalam saluran tak simetri berliang dipertimbangkan. Penyelesian tepat untuk rangkap arus, kecerunan tekanan membujur, halaju membujur, tegasan ricih, medan suhu dan medan kepekatan diperoleh dengan menggunakan penghampiran panjang gelombang yang panjang dan nombor Reynold yang kecil. Keputusan menunjukkan peristalsis mengepam dan memerangkap bendalir berkurangan apabila meningkatnya parameter halaju gelinciran. Seterusnya, suhu meningkat dengan peningkatan parameter haba gelinciran. Tambahan pula, profil kepekatan menurun dengan meningkatnya parameter keliangan, nombor Schmidt dan parameter kepekatan gelinciran. Perbandingan dengan keputusan yang telah diterbitkan menunjukkan persetujuan yang baik.

Kata kunci: Aliran peristalsis MHD; gelincir separa; medium berliang; memerangkap; mengepam; pemindahan haba dan jisim

INTRODUCTION

It is a fact that the peristaltic waves induced by the boundaries of channel or tube have a key role for fluid transport in the living organisms and in industrial pumping. The peristaltic activity is quite familiar in the gastrointestinal tract, bile ducts, the ureter, the esophagus and other glandular ducts. Roller and finger pumps also function under this mechanism. The peristalsis in the presence of heat transfer is imperative in many processes as oxygenation and hemodialysis. Heat transfer is also significant in the treatment of diseased tissues in cancer. Furthermore, the human lungs, bile duct and gall bladder have stones that behave like natural porous media. Also, keeping in mind the pathological situations, the distribution of fatty cholesterol and artery clogging blood clots in the coronary artery may be considered as the domains of porous medium. The magnetohydrodynamic peristaltic flow in a channel has a pivotal role in the motion of physiological fluids including blood and blood pump machines. Mass transfer in peristaltic flow occurs during the chemical breakdown of food, amalgamation of gastric juices with food and in other digestion processes. Motivated by these facts, several theoretical and experimental attempts have been made in view of the practical applications of peristalsis since the first investigation of Latham (1966). Few representative investigations on the topic may include the recent works through the studies (Akbar & Nadeem 2011; Elmaboud & Mekheimer 2011; Hayat & Mehmood 2011; Hayat & Noreen 2010; Hayat et al. 2010a; Mahmoud 2011; Mahmoud et al. 2011; Mehmood et al. 2013; Mekheimer & Elmaboud 2008; Muthuraj & Srinivas 2010a; Sezer & Yildirim 2010; Shafie et al. 2013; Srinivas & Muthuraj 2010).

Yildirim and Sezer (2010) considered the effects of partial slip on peristaltic flow of MHD viscous fluid in an asymmetric channel. They found that for positive flow rate the pressure rise decreases with increasing velocity slip parameter. Furthermore, slip effects on the MHD peristaltic flow in an asymmetric channel with heat transfer were examined by Nadeem and Akram (2010). They obtained the solutions by Adomian decomposition method and noted that the trapping reduces with the

increasing velocity slip parameter. Hayat et al. (2010b) investigated the simultaneous effects of slip and heat transfer on peristaltic flow in an asymmetric channel. They observed that the temperature is an increasing function of thermal slip parameter and decreasing function of phase difference. Muthuraj and Srinivas (2010b) studied the mixed convective heat and mass transfer in a porous vertical wavy channel by taking into account the no-slip conditions. Moreover, Srinivas et al. (2011) studied the mixed convective heat and mass transfer on peristaltic flow in an asymmetric channel subject to no-slip conditions. They concluded that the concentration decreases with an increase in flow rate and channel width ratio while concentration increases with increasing Soret number and phase difference.

To the best of our knowledge, no existing attempt highlights the slip effects on the MHD peristaltic flow in an asymmetric channel with porous medium and heat and mass transfer. No doubt, the fluid exhibits slip effects when mean free path length of the fluid is comparable to the distance between the plates as in nanochannels or microchannels. The main objective here was to study the slip and mass transfer effects on peristaltic flow in an asymmetric channel. Hence the solution expressions are first derived for long wavelength and low Reynolds number and then analyzed in details. The phenomenan of pumping and trapping have been accorded enough attention.
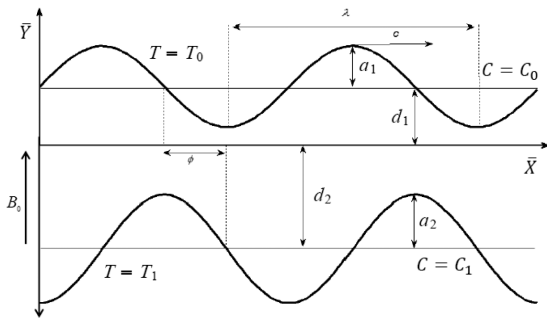
MATHEMATICAL ANALYSIS

FIGURE 1. Sketch of the physical model

Consider the two-dimensional flow of a viscous fluid in an asymmetric channel having width $d_1 + d_2$. An incompressible fluid fills the porous space. We choose the Cartesian coordinate system with $\bar{X}$-axis along the centerline in the direction of wave propagation and $\bar{Y}$-axis transverse to it. We assume sinusoidal wave propagating with constant velocity c along the walls of the channel. The sketch of the physical model is given in Figure 1. Since the peristaltic motion is sinusoidal in nature (Latham 1966), the channel walls have been represented through the following shapes:

$$\bar{H}_1\left(\bar{X},\bar{t}\right) = d_1 + a_1\sin\left[\frac{2\pi}{\lambda}\left(\bar{X}-c\bar{t}\right)\right], \quad \text{at upper wall,} \quad (1)$$

$$\bar{H}_2\left(\bar{X},\bar{t}\right) = -d_2 - a_2\sin\left[\frac{2\pi}{\lambda}\left(\bar{X}-c\bar{t}\right)+\phi\right], \quad \text{at lower wall,} \quad (2)$$

where $a_i(i=1,2)$ are the amplitudes of waves at upper and lower walls, respectively, λ is the wave length, $\bar{t}$ is the time, ϕ is the phase difference varying in the range $0 \le \phi \le \pi$ where $\phi = 0$ corresponds to the channel with waves out of phase and for $\phi = \pi$, the waves are in phase. Furthermore, the geometry parameters satisfy the relation,

$$a_1^2 + a_2^2 + 2a_1a_2\cos\phi \le \left(d_1+d_2\right)^2. \quad (3)$$

The upper wall is maintained at the temperature T_0 and concentration C_0 while the lower wall is maintained at temperature T_1 and concentration C_0. The fluid is electrically conducting in the presence of constant magnetic field $\mathbf{B_0}$ applied in the transverse direction. The equations describing the two-dimensional flow are (Srinivas et al. 2011)

$$\frac{\partial\bar{U}}{\partial\bar{X}} + \frac{\partial\bar{V}}{\partial\bar{Y}} = 0, \quad (4)$$

$$\rho\left(\frac{\partial}{\partial\bar{t}} + \bar{U}\frac{\partial}{\partial\bar{X}} + \bar{V}\frac{\partial}{\partial\bar{Y}}\right)\bar{U} = -\frac{\partial\bar{P}}{\partial\bar{X}} + \mu\left(\frac{\partial^2\bar{U}}{\partial\bar{X}^2} + \frac{\partial^2\bar{U}}{\partial\bar{Y}^2}\right)$$
$$-\chi B_0^2\bar{U} - \frac{\mu}{\bar{K}}\bar{U}, \quad (5)$$

$$\rho\left(\frac{\partial}{\partial\bar{t}} + \bar{U}\frac{\partial}{\partial\bar{X}} + \bar{V}\frac{\partial}{\partial\bar{Y}}\right)\bar{V} = -\frac{\partial\bar{P}}{\partial\bar{Y}} + \mu\left(\frac{\partial^2\bar{V}}{\partial\bar{X}^2} + \frac{\partial^2\bar{V}}{\partial\bar{Y}^2}\right)$$
$$-\frac{\mu}{\bar{K}}\bar{V}, \quad (6)$$

$$\rho\xi\left(\frac{\partial}{\partial\bar{t}} + \bar{U}\frac{\partial}{\partial\bar{X}} + \bar{V}\frac{\partial}{\partial\bar{Y}}\right)T = k\nabla^2 T$$
$$+\mu\left\{\left(\frac{\partial^2\bar{U}}{\partial\bar{Y}} + \frac{\partial^2\bar{V}}{\partial\bar{X}}\right)^2 + 2\left(\left(\frac{\partial\bar{U}}{\partial\bar{X}}\right)^2 + \left(\frac{\partial\bar{V}}{\partial\bar{Y}}\right)^2\right)\right\}, \quad (7)$$

$$\left(\frac{\partial}{\partial\bar{t}} + \bar{U}\frac{\partial}{\partial\bar{X}} + \bar{V}\frac{\partial}{\partial\bar{Y}}\right)C = D\nabla^2 C + \frac{DK_T}{T_m}\left(\frac{\partial^2 T}{\partial\bar{X}^2} + \frac{\partial^2 T}{\partial\bar{Y}^2}\right), \quad (8)$$

where ρ is the fluid density, $\bar{U}$ and $\bar{V}$ are the velocity components along $\bar{X}$ and $\bar{Y}$ directions, respectively, $\bar{P}$ is the pressure, μ is the dynamic viscosity of the fluid, χ is the electrical conductivity of fluid, k is the thermal conductivity, $\bar{K}$ is the permeability parameter, ξ is the specific heat at constant volume, T and C are the temperature and concentration of fluid, D is the coefficient of mass diffusivity, T_m is the mean temperature and K_T is the thermal-diffusion ratio.

We choose a wave frame $(\bar{x}, \bar{y})$ moving with the velocity c away from the laboratory frame $(\bar{X}, \bar{Y})$. The transformations in the two frames are taken as

$$\bar{x} = \bar{X} - c\bar{t}, \ \bar{y} = \bar{Y}, \ \bar{u} = \bar{U} - c, \ \bar{v} = \bar{V}, \ \bar{p}(\bar{x}, \bar{y}) = P(\bar{X}, \bar{Y}, \bar{t}),$$

$$(9)$$

where $(\bar{u}, \bar{v})$ are the longitudinal and transverse components of velocity in the wave frame $(\bar{x}, \bar{y})$ and $\bar{p}$ is the pressure. Using transformations (9) along with the variables

$$x = \frac{\bar{x}}{\lambda}, \quad y = \frac{\bar{y}}{d_1}, \quad u = \frac{\bar{u}}{c}, \quad v = \frac{\bar{v}}{c}, \ t = \frac{c}{\lambda}\bar{t}, \ p = \frac{d_1^2}{\lambda \mu c}\bar{p},$$

$$h_1 = \frac{\bar{H}_1}{d_1}, \ h_2 = \frac{\bar{H}_2}{d_1}, \ \delta = \frac{d_1}{\lambda}, \ R = \frac{\rho c d_1}{\mu}, \ M^2 = \frac{\chi}{\mu}B_0^2 d_1^2,$$

$$\eta = \frac{T - T_0}{T_1 - T_0}, \ \ \mathrm{Pr} = \frac{\rho \nu \xi}{k}, \ \ \varphi = \frac{C - C_0}{C_1 - C_0}, \ \ E = \frac{c^2}{\xi(T_1 - T_0)},$$

$$K = \frac{\bar{K}}{d_1^2}, \ \ Sc = \frac{\mu}{\rho D}, \ \ Sr = \frac{\rho D K_T (T_1 - T_0)}{\mu T_m (C_1 - C_0)}, \ Br = \mathrm{Pr}\, E,$$

$$(10)$$

$$u = \frac{\partial \Psi}{\partial y}, \ v = -\delta \frac{\partial \Psi}{\partial x},$$

$$(11)$$

we have after utilizing the long wavelength approximation and low Reynolds number the following expressions,

$$\frac{\partial^4 \Psi}{\partial y^4} = \left(M^2 + \frac{1}{K}\right)\frac{\partial^2 \Psi}{\partial y^2},$$

$$(12)$$

$$\frac{dp}{dx} = \frac{\partial^3 \Psi}{\partial y^3} - \left(M^2 + \frac{1}{K}\right)\left(\frac{\partial \Psi}{\partial y} + 1\right),$$

$$(13)$$

$$\frac{\partial^2 \eta}{\partial y^2} + Br\left(\frac{\partial^2 \Psi}{\partial y^2}\right)^2 = 0,$$

$$(14)$$

$$\frac{1}{Sc}\frac{\partial^2 \varphi}{\partial y^2} + Sr\frac{\partial^2 \eta}{\partial y^2} = 0,$$

$$(15)$$

and $p \neq p\,(y)$. In above expressions, M is the Hartman number, Br is the Brinkman number, Sc is the Schmidt number and Sr is the Soret number.

The boundary conditions are taken (Hayat et al. 2010b) in the forms as,

$$\Psi = \frac{F}{2}, \frac{\partial \Psi}{\partial y} + \beta \frac{\partial^2 \Psi}{\partial y^2} = -1, \ \eta + \gamma \frac{\partial \eta}{\partial y} = 0,$$

$$\varphi + \sigma \frac{\partial \varphi}{\partial y} = 0 \ \ \text{at} \ \ y = h_1(x),$$

$$(16)$$

$$\Psi = -\frac{F}{2}, \frac{\partial \Psi}{\partial y} + \beta \frac{\partial^2 \Psi}{\partial y^2} = -1, \ \eta - \gamma \frac{\partial \eta}{\partial y} = 1,$$

$$\varphi - \sigma \frac{\partial \varphi}{\partial y} = 1 \ \ \text{at} \ \ y = h_2(x),$$

$$(17)$$

$$h_1(x) = 1 + a \sin(2\pi x), \quad h_2(x) = -d - b \sin(2\pi x + \phi),$$

$$(18)$$

with $a = a_1/d_1, b = a_2/d_1, d = d_2/d_1$ and $a^2 + b^2 + 2ab \cos \phi \le (1 + d)^2$ and β is the dimensionless velocity slip parameter, γ is the dimensionless thermal slip parameter, σ is the dimensionless concentration slip parameter and F is the dimensionless average flux in the wave frame defined by,

$$F = \int_{h_2(x)}^{h_1(x)} \frac{\partial \Psi}{\partial y}\, dy = \Psi(h_1(x)) - \Psi(h_2(x)).$$

$$(19)$$

The exact solutions of (12) to (15) along with the boundary conditions (16) and (17) were obtained by direct integration and the results are generated using the software MATHEMATICA. The solutions of stream function Ψ, longitudinal velocity u, longitudinal pressure gradient dp/dx, shear stress at the upper wall $(y = h_1)\ S_{xy}$, temperature η and concentration field φ are

$$\Psi = S_1 + S_2 y + S_3 \cosh \sqrt{J} y + S_4 \sinh \sqrt{J} y,$$

$$(20)$$

$$u = S_2 + S_3 \sqrt{J} \sinh \sqrt{J} y + S_4 \sqrt{J} \cosh \sqrt{J} y,$$

$$(21)$$

$$\frac{dp}{dx} = -(1 + A_4)\, J,$$

$$(22)$$

$$S_{xy} = S_3 J \cosh \sqrt{J} h_1 + S_4 J \sinh \sqrt{J} h_1,$$

$$(23)$$

$$\eta = B_1 + B_2 y - L_{17} y^2 - L_{18} \cosh 2\sqrt{J} y - L_{19} \sinh 2\sqrt{J} y,$$

$$(24)$$

$$\varphi = C_1 + C_2 y + Sc\, Sr\{L_{17} y^2 + L_{18} \cosh 2\sqrt{J} y + L_{19} \sinh 2\sqrt{J} y\},$$

$$(25)$$

where

$$S_1 = A_3, \ \ S_2 = A_4, \ \ S_3 = (A_1 + A_2)/J,$$
$$S_4 = (A_1 - A_2)/J, \ \ J = M^2 + (1/K),$$

$$B_1 = \{L_1 A_1^2 + L_2 A_1 A_2 + L_3 A_2^2 + L_4\}/4J(h_1 - h_2 + 2\gamma)\},$$

$$B_2 = \{L_5 A_1^2 + L_6 A_1 A_2 + L_7 A_2^2 + L_8\}/4J(h_1 - h_2 + 2\gamma)\},$$

$$C_1 = \{L_9 A_1^2 + L_{10} A_1 A_2 + L_{11} A_2^2 + L_{12}\}/4J(h_1 - h_2 + 2\sigma)\},$$

$$C_2 = \{L_{13} A_1^2 + L_{14} A_1 A_2 + L_{15} A_2^2 + L_{16}\}/4J(h_1 - h_2 + 2\sigma)\},$$

and all the quantities involved in the above computations are presented in Appendix.

The non-dimensional pressure rise per wavelength (Δp_λ) and frictional forces $(F_{\lambda 1})$ and $(F_{\lambda 2})$ at the upper and lower walls are (Hayat & Mehmood 2011),

$$\Delta p_\lambda = \int_0^1 \frac{dp}{dx}\, dx, \quad F_{\lambda 1} = \int_0^1 -h_1^2 \frac{dp}{dx}\, dx, F_{\lambda 2} = \int_0^1 -h_2^2 \frac{dp}{dx}\, dx.$$

(26)

DIFFERENT WAVE FORMS

The non-dimensional expressions for different wave forms are represented by

Sinusoidal Wave:

$$h(x) = 1 + a \sin(2\pi x).$$ (27)

Triangular Wave:

$$h(x) = 1 + a\{ \frac{8}{\pi^3} \sum_{m=1}^{\infty} \frac{(-1)^{m+1}}{(2m-1)^2} \sin(2(2m-1)\pi x)\}.$$ (28)

Square Wave:

$$h(x) = 1 + a\{ \frac{4}{\pi} \sum_{m=1}^{\infty} \frac{(-1)^{m+1}}{(2m-1)^2} \cos(2(2m-1)\pi x)\}.$$ (29)

Trapezoidal Wave:

$$h(x) = 1 + a\{ \frac{32}{\pi^2} \sum_{m=1}^{\infty} \frac{\sin\frac{\pi}{8}(2m-1)}{(2m-1)^2} \sin(2(2m-1)\pi x)\}.$$

(30)

In the present study, the analysis was done by taking the first fifty terms of the above series.

DISCUSSION

PUMPING

The pumping characteristics for different values of slip parameter β were analyzed. The pressure rise has been computed first by numerical integration and then plots were presented. The regions of interest are peristaltic pumping region ($\Delta p_\lambda > 0$, $\theta > 0$), free pumping region ($\Delta p_\lambda = 0$, θ

> 0) and augmented pumping region ($\Delta p_\lambda < 0$, $\theta > 0$). The comparison of the present series solution for pressure rise per wave length Δp_λ for different flow rate θ is presented in Figure 2. These results are found in good agreement with those reported by Mishra and Rao (2003).
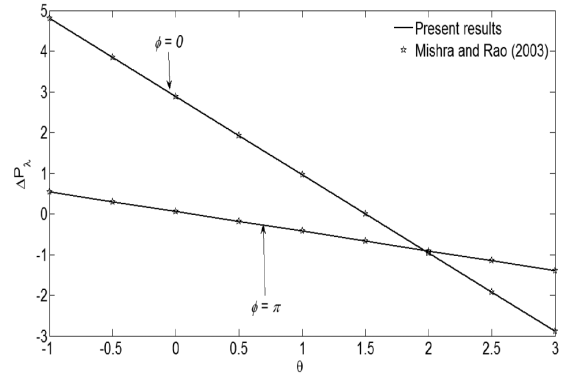
FIGURE 2. Comparison of pressure rise per wavelength Δp_λ for different flow rate θ when $d = 2$, $a = 0.7$, $b = 1.2$, $\mathrm{K} \to \infty, \mathrm{M} = 0, \beta = 0$

The slip effects on dimensionless pressure rise per wave length Δp_λ against the dimensionless average flux θ is shown in Figure 3(a). Both peristaltic and free pumping decreases when β increases which shows that the velocity slip reduces the efficiency of the peristaltic and free pumping. However, the augmented pumping decreases for $\theta < 1.4$ and increases when $\theta > 1.4$. Physically, velocity slip lessens the strength of augmented pumping below a critical value of $\theta = 1.4$, after this critical value the augmented pumping is enhanced with an increase in velocity slip parameter.

In Figure 3(b) Δp_λ against θ for different wave forms (triangular, sinusoidal, trapezoidal and square) is sketched. It was found that in peristaltic pumping and free pumping, the square wave gives best pumping characteristics and triangular wave gives worst pumping characteristics. In augmented pumping such behaviour is inverted after $\theta = 1.3$. The longitudinal pressure gradient
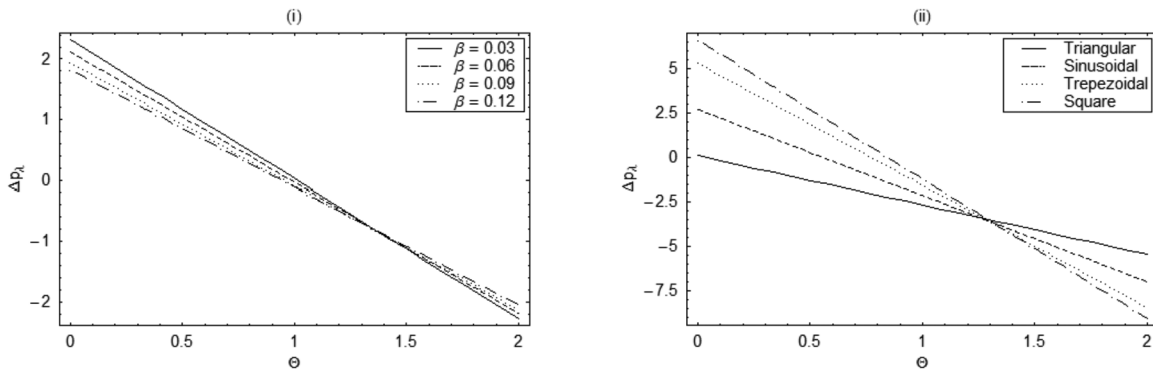
FIGURE 3. Pressure rise Δp_λ for (a) β with $d = 2$, $a = 0.7$, $b = 1.2$, $\phi = \frac{\pi}{4}$, $K = 1$, $\mathrm{M} = 1$, (b) different wave forms versus θ when $d = 1$, $a = 0.5$, $b = 0.5$, $\phi = 0$, $K = 1$, $M = 1$, $\beta = 0$

dp/dx for different values of slip parameter β is shown in Figure 4. It was noticed that dp/dx decreases with an increase in β and meets its maxima in the interval $x \in [0.4,1]$ where it resists the flow.
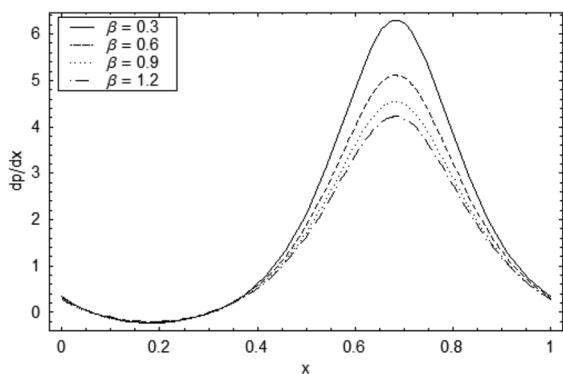

FIGURE 4. Pressure gradient dp/dx against x for β with $d = 2$, $a = 0.7, b = 0.8, \phi = \frac{\pi}{4}$, $K = 1, M = 1, F = -4$

SHEAR STRESS

The shear stress distribution S_{xy} (via x) on the upper wall ($y = h_1$) is shown in Figure 5 for various values of β. Oscillatory behaviour in view of the peristaltic waves along the walls is noticed. The absolute value of shear stress S_{xy} is a decreasing function of β which depicts that as the velocity slip parameter become greater in magnitude, the shear stress becomes weaken along the walls of the channel.

FRICTIONAL FORCES

The variation of slip parameter on the frictional forces at lower and upper walls is seen by numerical integration over the domain [0,1]. In Figure 6(a) frictional force $F_{\lambda1}$ is plotted against θ for different values of β at the upper wall ($y = h_1$). Through an increase in β there exists a critical value of θ below which $F_{\lambda1}$ increases and resists the flow, above this critical value the behaviour is opposite and $F_{\lambda1}$ decreases and assists the flow. Similar qualitative behaviour is found for $F_{\lambda2}$ at lower wall ($y = h_2$) in Figure 6(b).
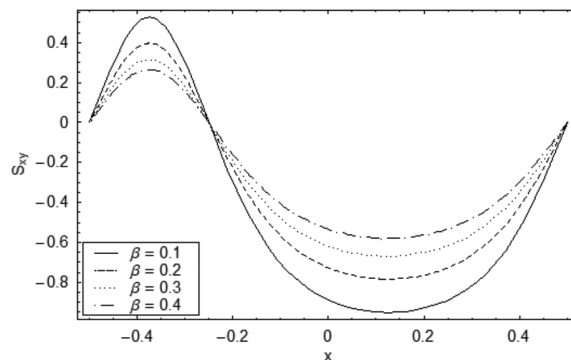

FIGURE 5. Shear Stress S_{xy} against x for β with $d = 1, a = 0.5$, $b = 0.5$, $\phi = \frac{\pi}{2}$, $K = 1, F = -1.5$

VELOCITY PROFILE

The behaviour of β on longitudinal velocity component u in symmetric and asymmetric channels at cross section $x = 0.5$ is sketched in Figure 7. Figure 7(a) depicts the variation of u versus transverse coordinate y for symmetric channel ($f = 0$). Here, u increases near the walls when β increases but near the centerline u decreases. Figure 7(b) is plotted for asymmetric channel $\left(\phi = \frac{\pi}{6}\right)$ and the qualitative behaviour is found the same but quantitatively, the magnitude of u increases in case of asymmetric channel.

TEMPERATURE PROFILE

Figure 8 highlights the variations of β and γ on the temperature distribution η plotted against y. Here η decreases when β increases. Further η increases with an increase in γ. The temperature profile is almost parabolic and the temperature is greater in magnitude in lower portion of the channel.

CONCENTRATION PROFILE

Concentration distribution φ is observed at the cross section $x = 0.2$ of the channel. The solution φ is plotted for different values of Br, K, Sc, σ, M and β in Figure 9. We note that φ decreases with an increase in Br, K, Sc and
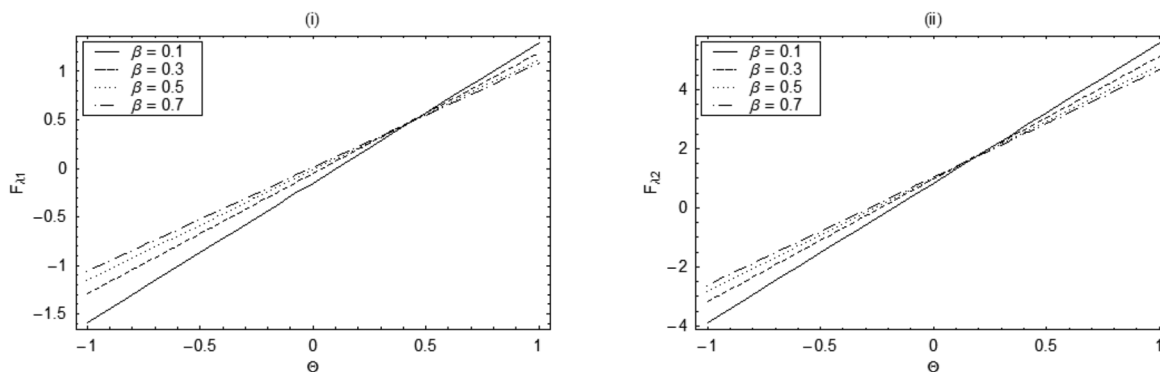

FIGURE 6. Frictional forces $F_{\lambda1}$ (i) and $F_{\lambda2}$ (ii) for β with fixed $d = 2, a = 0.7, b = 1.2$, $\phi = \frac{3\pi}{2}$, $K = 1, M = 1$
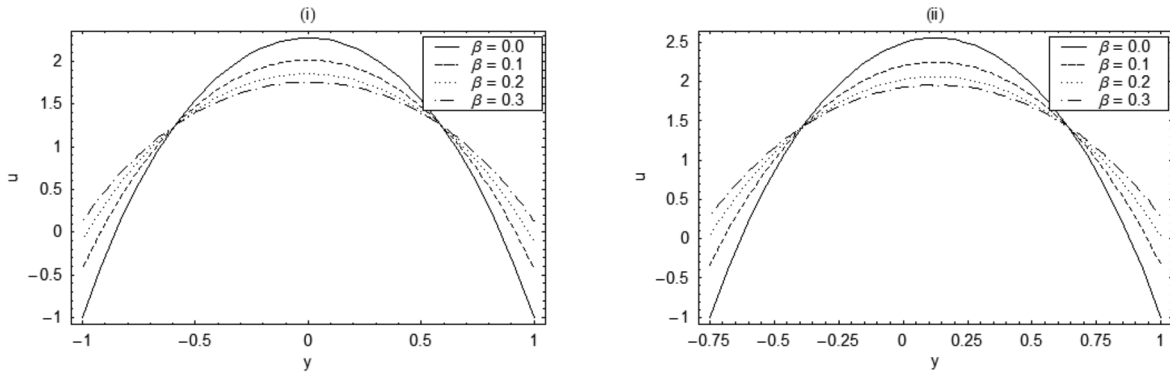
FIGURE 7. Velocity profile u with y for β when $d = 1, a = 0.5, b = 0.5, F = 2.5, K = 1, x\,0.5, M = 1, (i)\phi = 0 (ii)\,\phi = \dfrac{\pi}{6}$
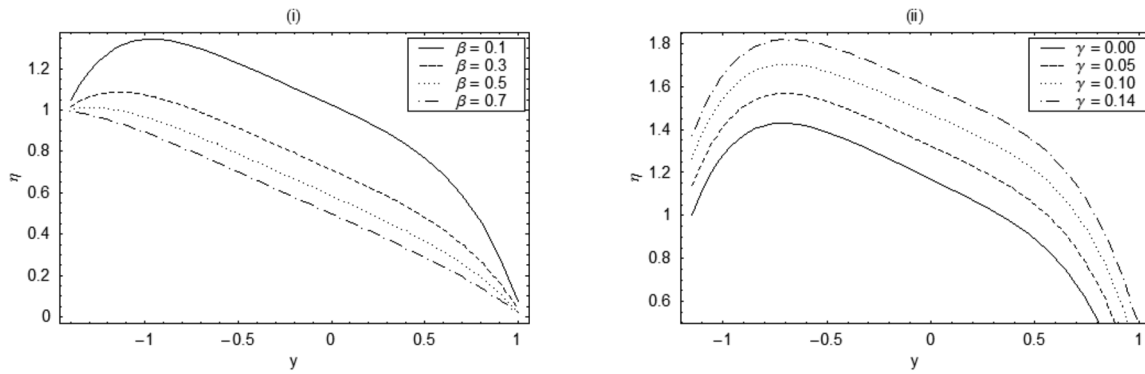

FIGURE 8. Temperature profile η with y when $d = 2, b = 1.2, x = 0.5, M = 1, F = -1, Br = 4$
(i) $a = 0.7, \phi = \frac{\pi}{6}, K = 2, \gamma = 0.03$, (ii) $a = 0.9, \phi = \frac{\pi}{4}, \beta = 0.01, K = 1$

σ. Moreover, φ is an increasing function of M and β. The concentration distribution is found almost parabolic and is greater in magnitude below the centerline of the channel. The variations are less near the walls in comparison to the centerline of channel.

TRAPPING

Here for symmetric channel ($f = 0$) the stream lines are plotted for sinusoidal, triangular, square and trapezoidal waveforms in Figures 10 to 13. Panel (a) was plotted for no-slip case $\beta = 0$ and panels (b) and (c) were made when $\beta \neq 0$. For no-slip case two equal circulating trapped bolus exists near both upper and lower walls and with an increase in β, this circulation of fluid decreases equally and symmetrically while the trapping vanishes for large β. The stream lines for sinusoidal waveform were plotted for the asymmetric channel $\left(\phi = \frac{\pi}{2}\right)$ in Figure 14. These figures exhibit that the trapping exist for both lower and upper walls but not symmetric along the centerline and the trapping reduces sharply below the centerline of the channel when β increases.

CONCLUSION

This study waas devoted to the slip effects and mass transfer on peristaltic flow in an asymmetric channel.

Analysis has been carried out for different wave forms. It was observed that the peristaltic and free pumping decrease by increasing velocity slip parameter. The square wave gave the highest pumping rate in peristaltic and free pumping cases. Longitudinal velocity subject to the slip effects has opposite behaviour at the centerline and near the channel walls. The circulation of trapped bolus vanishes for large velocity slip parameter. An increase in thermal slip parameter results in the increase of temperature. Concentration profile is a decreasing function of Brinkman number, porosity parameter and Schmidt number. The velocity and concentration slip parameters have opposite effects on concentration profile.

APPENDIX

Here we present the values involved in the solution expressions. These are

$$L_1 = -Br((h_2 - 2\gamma + 2\sqrt{J}\,h_2\gamma + h_1(-1 + 2\sqrt{J}\,\gamma))\cosh\sqrt{J}$$
$$(h_1 - h_2) + (h_1 + h_2 - 2\sqrt{J}\,h_1\gamma + 2\sqrt{J}\,h_2\gamma - 4\sqrt{J}\,\gamma^2)\sinh$$
$$\sqrt{J}\,(h_1 - h_2)(\cosh\sqrt{J}\,(h_1 + h_2) + \sinh\sqrt{J}\,(h_1 + h_2),$$

$$L_2 = -4\sqrt{J}\,Br(h_1 - h_2 + 2\gamma)h_1)h_2 - \gamma) + h_2\gamma),$$

$$L_3 = Br((h_1 + \gamma)(1 + 2\sqrt{J}\,\gamma)(\cosh 2\sqrt{J}\,h_1 + \sinh 2\sqrt{J}\,h_1)$$
$$+ (h_2 - \gamma)(-1 + 2\sqrt{J}\,\gamma)(\cosh 2\sqrt{J}\,h_2 + \sinh 2\sqrt{J}\,h_2))$$
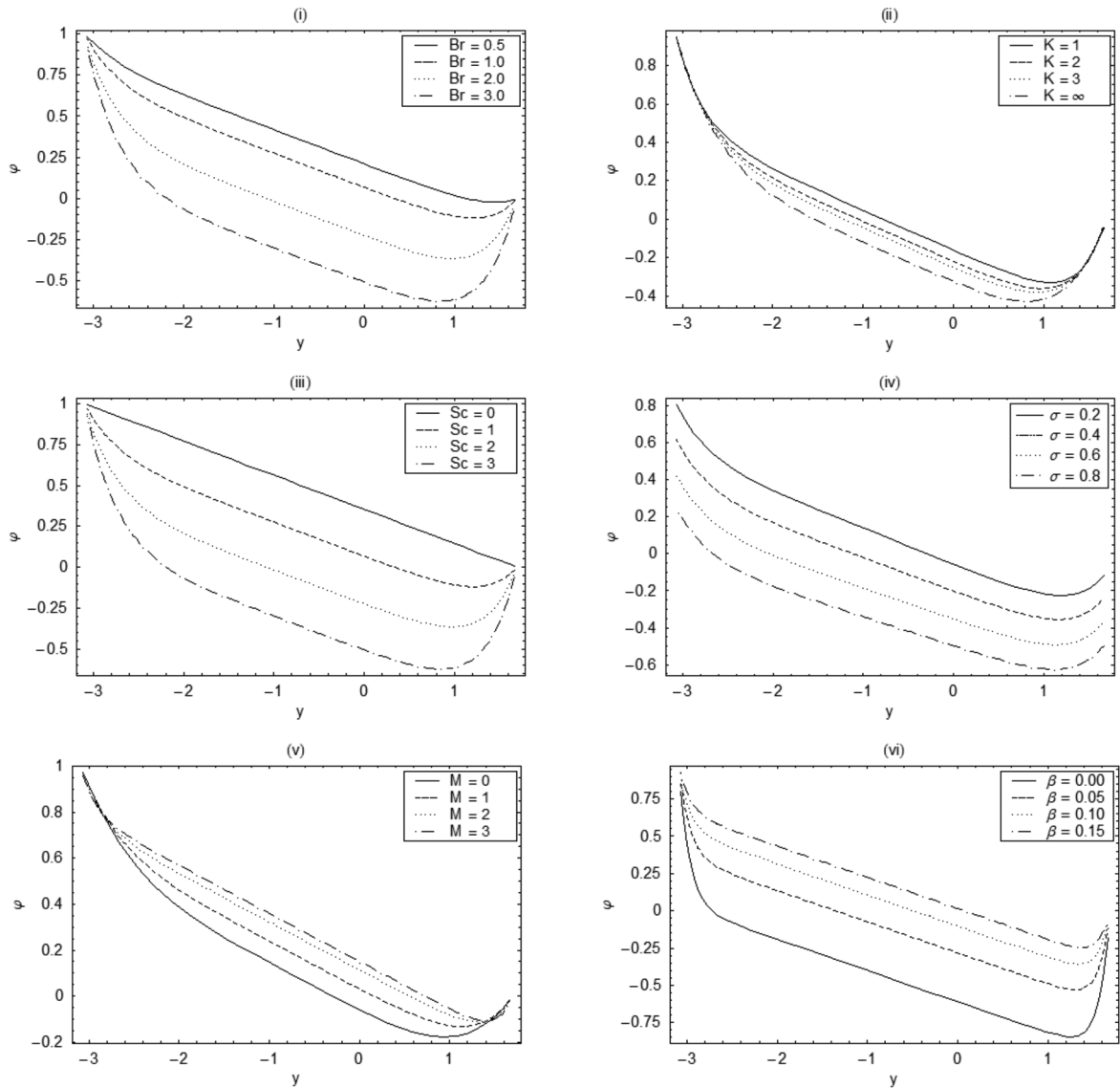$$(\cosh 2\sqrt{J}\,(h_1 + h_2) - \sinh 2\sqrt{J}\,(h_1 + h_2)),$$

FIGURE 9. Concentration profile φ with y for $d = 2$, $a = 0.7$, $b = 1.2$, $F = -1$, $x = 0.2$, $\phi = \pi/4$, $Sr = 1$, (*i*) $\beta = 0.03$, $\gamma = 0.03$, $K = 1$, $\sigma = 0.03$, $Sc = 1$, $M = 1$, (*ii*) $\beta = 0.03$, $\gamma = 0.03$, $Br = 2$, $\sigma = 0.03$, $Sc = 1$, $M = 1$, (*iii*) $\beta = 0.03$, $\gamma = 0.03$, $Br = 1$, $\sigma = 0.03$, $K = 1$, $M = 1$, (*iv*) $\beta = 0.03$, $\gamma = 0.03$, $Br = 1$, $K = 1$, $Sc = 1$, $M = 1$, (*v*) $\beta = 0.03$, $\gamma = 0.03$, $Br = 1$, $\sigma = 0.03$, $K = 1$, $Sc = 1$, (*vi*) $Br = 1$, $\gamma = 0.03$, $M = 1$, $\sigma = 0.03$, $K = 1$, $Sc = 1$

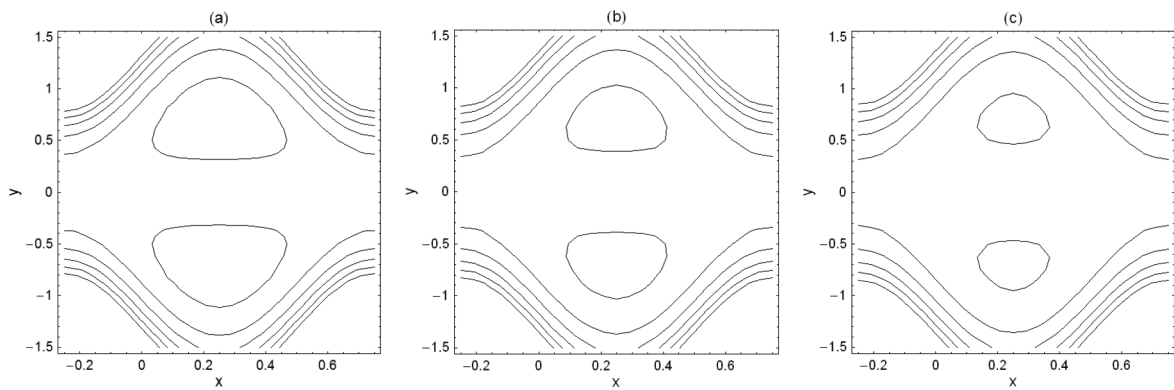

FIGURE 10. Stream lines with fixed $a = 0.5$, $b = 0.5$, $d = 1$, $\phi = -0.35$, $M = 1$, $K = 1$ and sinusoidal wave form (symmetric channel) for β (*a*) 0.00, (*b*) 0.05, (*c*) 0.09
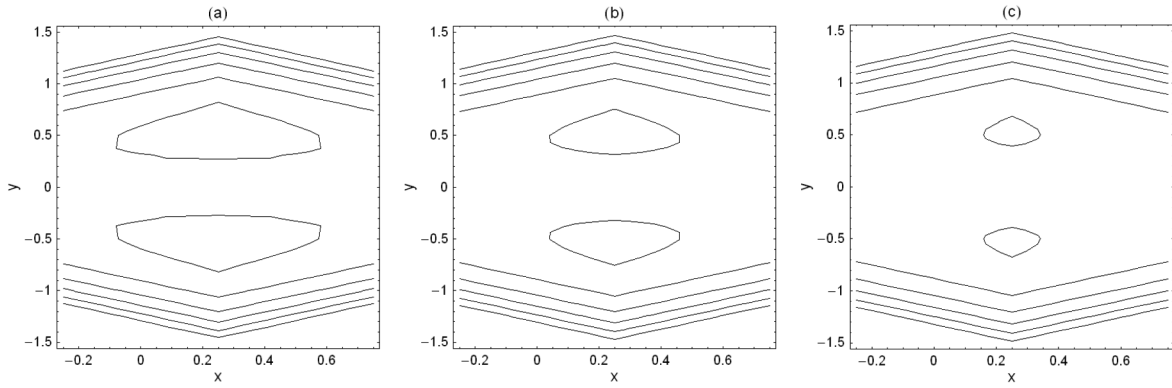
FIGURE 11. Stream lines with fixed $a = 0.5, b = 0.5, d = 1, \phi = 0, F = -0.35, M = 1, K = 1$ and triangular wave form (symmetric channel) for β (a) 0.00, (b) 0.03, (c) 0.06
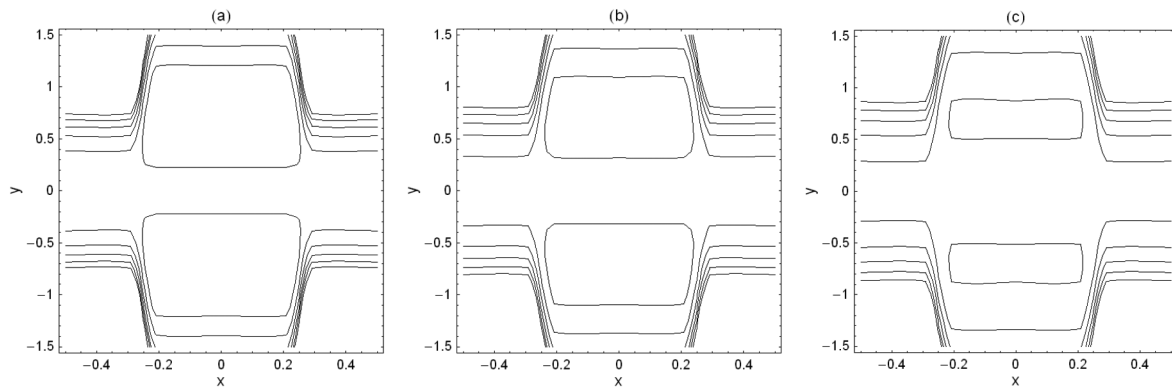

FIGURE 12. Stream lines with fixed $a = 0.5, b = 0.5, d = 1, \phi = 0, F = -0.30, M = 1, K = 1$ and square wave form (symmetric channel) for β (a) 0.00, (b) 0.10, (c) 0.22
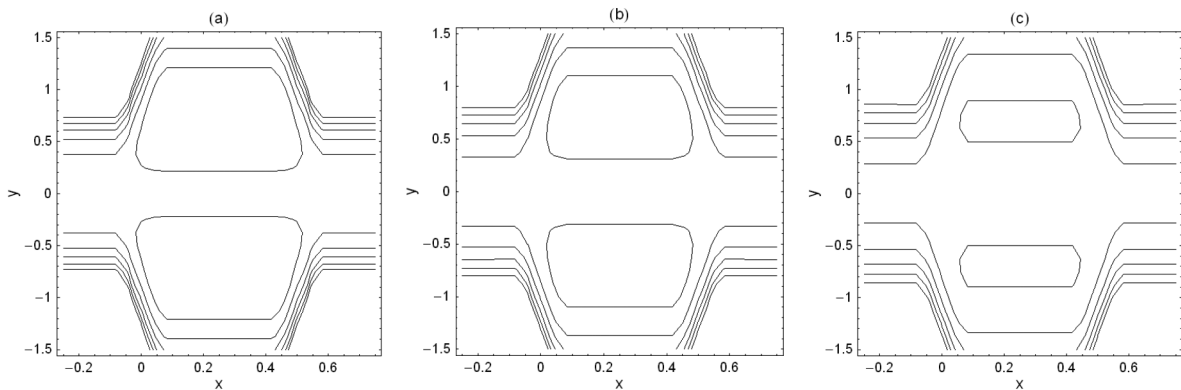

FIGURE 13. Stream lines with fixed $a = 0.5, b = 0.5, d = 1, \phi = 0, F = -0.30, M = 1, K = 1$ and trapezoidal wave form (symmetric channel) for β (a) 0.00, (b) 0.10, (c) 0.22

$L_4 = 4\sqrt{J}\,(\mathrm{h}1 + \gamma),$

$L_5 = 2Br(2\sqrt{J}\,\gamma \cosh\sqrt{J}\,(h_1 - h_2) + \sinh\sqrt{J}\,(h_1 - h_2))(\cosh\sqrt{J}\,(h_1 + h_2 + \sinh\sqrt{J}\,(h_1 + h_2)),$

$L_6 = 4\sqrt{J}\,Br(h_1 + h_2)(h_1 - h_2 + 2\gamma),$

$L_7 = -2Br(2\sqrt{J}\,\gamma\,\cosh\sqrt{J}\,(h_1 - h_2) + \sinh\sqrt{J}\,(h_1 - h_2))(\cosh\sqrt{J}\,(h_1 + h_2) - \sinh\sqrt{J}\,(h_1 + h_2)),$

$L_8 = -4\sqrt{J}\,,\ L_9 = BrScSr(\cosh 2\sqrt{J}\,(h_1 + h_2) - \sinh 2\sqrt{J}\,(h_1 + h_2))((h_2 - \sigma)(1 + 2\sqrt{J}\,\sigma)\cosh 2\sqrt{J}\,(2h_1 + h_2) + (h_1 + \sigma)(-1 + 2\sqrt{J}\,\sigma)\cosh 2\sqrt{J}\,(h_1 + 2h_2) + h_2\sinh 2\sqrt{J}\,(2h_1 + h_2) - \sigma\sinh 2\sqrt{J}\,(2h_1 + h_2) + 2\sqrt{J}\,h_2\sigma\sinh 2\sqrt{J}\,(2h_1 + h_2) - 2\sqrt{J}\,\sigma^2\sinh 2\sqrt{J}\,(2h_1 + h_2) - h_1\sinh 2\sqrt{J}\,\sigma^2\sinh 2\sqrt{J}\,(h_1 + 2h_2)),$
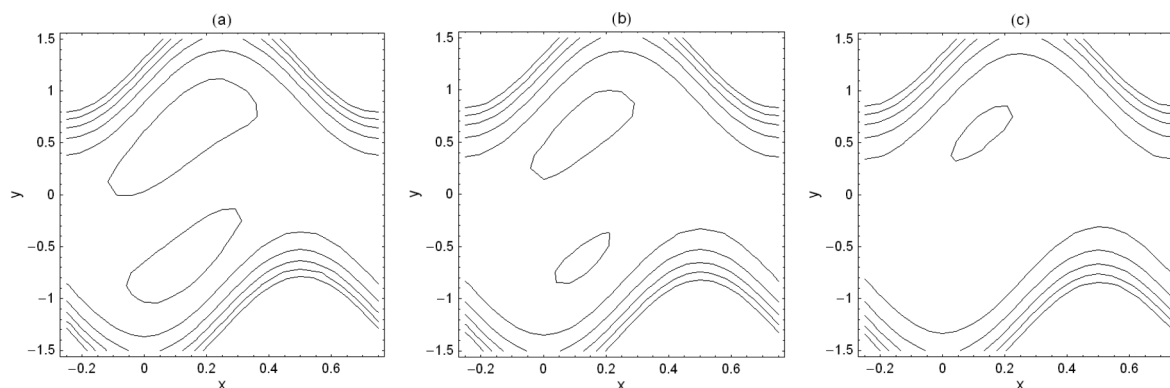
FIGURE 14. Stream lines with fixed $a = 0.5$, $b = 0.5$, $d = 1$, $\phi = \pi/2$, $F = -0.30$, $M = 1$, $K = 1$ and sinusoidal wave form (asymmetric channel) for β (a) 0.00, (b) 0.05, (c) 0.09

$L_{10} = 4\sqrt{J}\; BrScSr(h_1{}^2(h_2 - \sigma) - h_2(h_2 - 2\sigma)\sigma - h_1(h_2{}^2 - 4h_2\sigma + 2\sigma^2))$,

$L_{11} = -BrSrSr(h_1 + \sigma)(1 + 2\sqrt{J}\,\sigma)\cosh 2\sqrt{J}\,h_1 + (h_2 - \sigma)(-1 + 2\sqrt{J}\,\sigma)\cosh 2\sqrt{J}\,h_2 + h_1 \sinh 2\sqrt{J}\,h_1 + \sigma \sinh 2\sqrt{J}\,h_1 + 2\sqrt{J}\,h_1\sigma \sinh 2\sqrt{J}\,h_1 + 2\sqrt{J}\,\sigma^2 \sinh 2\sqrt{J}\,h_1 - h_2 \sinh 2\sqrt{J}\,h_2 + \sigma \sinh 2\sqrt{J}\,h_2 + \sqrt{J}\,h_2\,\sigma \sinh 2\sqrt{J}\,h_2 - 2\sqrt{J}\,\sigma^2 \sinh 2\sqrt{J}\,h_2)(\cosh 2\sqrt{J}\,(h_1 + h_2) - \sinh 2\sqrt{J}\,(h_1 + h_2))$,

$L_{12} = 4\sqrt{J}\,(h_1 + \sigma)$,

$L_{13} = -2BrScSr(2\sqrt{J}\,\sigma \cosh \sqrt{J}\,(h_1 - h_2) + \sinh \sqrt{J}\,(h_1 - h_2))(\cosh \sqrt{J}\,(h_1 + h_2) + \sinh \sqrt{J}\,(h_1 + h_2))$,

$L_{14} = -4\sqrt{J}\,Br(h_1 + h_2)ScSr(h_1 - h_2 + 2\sigma)$,

$L_{15} = 2BrScSr(2\sqrt{J}\,\sigma \cosh \sqrt{J}\,(h_1 - h_2) + \sinh \sqrt{J}\,(h_1 - h_2))(\cosh \sqrt{J}\,(h_1 + h_2) - \sinh \sqrt{J}\,(h_1 + h_2))$,

$L_{16} = -4\sqrt{J}$,

$L_{17} = A_1 A_2 Br$,

$L_{18} = Br\{(A_1{}^2 + A_2{}^2)/(4\sqrt{J})\}$,

$L_{19} = Br\{(A_1{}^2 - A_2{}^2)/(4\sqrt{J})\}$,

$A_1 = \{-((F + h_1 - h_2)J)\}/\{(((-2 + \sqrt{J}\,(h_1 - h_2) + J(h_1 - h_2)\beta)\cosh \sqrt{J}\,h_1 + \sinh \sqrt{J}\,h_1) + ((2 + \sqrt{J}\,(h_1 - h_2) + J(-h_1 + h_2)\beta)(\cosh \sqrt{J}\,h_2 + \sinh \sqrt{J}\,h_2)\}$,

$A_2 = \{-((F_0 + h_1 - h_2)J(\cosh \sqrt{J}\,(h_1 + h_2) + \sinh \sqrt{J}\,(h_1 + h_2)))\}/\{(((2 + \sqrt{J}\,(-h_1 + h_2) + J(-h_1 + h_2)\beta)(\cosh \sqrt{J}\,h_1 + \sinh \sqrt{J}\,h_1) + ((-2 + \sqrt{J}\,(-h_1 + h_2) + J(h_1 - h_2)\beta)(\cosh \sqrt{J}\,h_2 + \sinh \sqrt{J}\,h_2)\}$

$A_3 = \{((h_1 + h_2)((2 + F\sqrt{J} + FJ\beta)(\cosh \sqrt{J}\,h_1 + \sinh \sqrt{J}\,h_1) + (-2 + F\sqrt{J} - FJ\beta)(\cosh \sqrt{J}\,h_2 + \sinh \sqrt{J}\,h_2)))\}/\{(2((2 + \sqrt{J}\,(-h_1 + h_2) + J(-h_1 + h_2)\beta)\cosh \sqrt{J}\,h_1 + \sinh \sqrt{J}\,Jh_1) + ((-2 + \sqrt{J}\,(-h_1 + h_2) + J(h_1 - h_2)\beta(\cosh \sqrt{J}\,h_2 + \sinh \sqrt{J}\,h_2)))\}$

$A_4 = \{((2 + F\sqrt{J} + FJ\beta)(\cosh \sqrt{J}\,h_1 + \sinh \sqrt{J}\,h_1) + (-2 + F\sqrt{J} - FJ\beta)(\cosh \sqrt{J}\,h_2 + \sinh \sqrt{J}\,h_2))\}/\{((-2 + \sqrt{J}\,(h_1 - h_2) + J(h_1 - h_2)\beta)(\cosh \sqrt{J}\,h_1 + \sinh \sqrt{J}\,h_1) + (2 + \sqrt{J}\,(h_1 - h_2) + J(-h_1 + h_2)\beta)(\cosh \sqrt{J}\,h_2 + \sinh \sqrt{J}\,h_2)$

REFERENCES

Akbar, N.S. & Nadeem, S. 2011. Simulation of heat transfer on the peristaltic flow of a Jeffrey-six constant fluid in a diverging tube. *International Communications in Heat and Mass Transfer* 38: 154-150.

Elmaboud, Y.Abd. & Mekheimer, Kh.S. 2011. Non-linear peristaltic transport of a second-order fluid through a porous medium. *Applied Mathematical Modelling* 35: 2695-2710.

Hayat, T. & Noreen, S. 2010. Peristaltic transport of fourth grade fluid with heat transfer and induced magnetic field. *Comptes Rendus Mecanique* 338: 518-528.

Hayat, T. & Mehmood, O.U. 2011. Slip effects on MHD flow of third order fluid in a planar channel. *Communications in Nonlinear Science and Numerical Simulation* 16: 1363-1377.

Hayat, T., Asghar, Z., Asghar, S. & Mesloub, S. 2010a. Influence of inclined magnetic field on peristaltic transport of fourth grade fluid in an inclined asymmetric channel. *Journal of the Taiwan Institute of Chemical Engineers* 41: 553-563.

Hayat, T., Hina, S. & Ali, N. 2010b. Simultaneous effects of slip and heat transfer on the peristaltic flow. *Communications in Nonlinear Science and Numerical Simulation* 15: 1526-1537.

Latham, T.W. 1966. Fluid motion in peristaltic pumps. MS Thesis, MIT (unpublished).

Mahmoud, S.R. 2011. Effect of rotation and magnetic field through porous medium on peristaltic transport of a Jeffrey fluid in tube. *Mathematical Problems in Engineering* 2011: 971456.

Mahmoud, S.R., Afifi, N.A. & Al-Isede, H.M. 2011. Effect of porous media and magnetic field on peristaltic transport of a Jeffrey fluid in an asymmetric channel. *International Journal of Mathematical Analysis* 5(21): 1025-1034.

Mehmood, O.U., Mustapha, N., Shafie, S. & Qasim, M. 2013. Dissipative heat transfer in peristaltic flow of Sisko fluid through a cylindrical tube with nonlinear slip. *Heat Transfer Research* (in press).

Mekheimar, Kh.S. & Elmaboud, Y.Abd. 2008. The influence of heat transfer and magnetic field on the peristaltic transport of Newtonian fluid in vertical annulus-Applications of an endoscope. *Physics Letter A* 372: 1657-1665.

Mishra, M. & Rao, A.R. 2003. Peristaltic flow of Newtonian fluid in an asymmetric channel. *Zeitschrift für angewandte Mathematik und Physik* 54: 532-550.

Muthuraj, R. & Srinivas, S. 2010a. A note on heat transfer to MHD oscillatory flow in an asymmetric wavy channel. *International Communications in Heat and Mass Transfer* 37: 1255-1260.

Muthuraj, R. & Srinivas, S. 2010b. Mixed convective heat and mass transfer in a vertical wavy channel with traveling thermal waves and porous medium. *Computers & Mathematics with Applications* 59: 3516-3528.

Nadeem, S. & Akram, S. 2010. Heat transfer in a peristaltic flow of MHD fluid with partial slip. *Communications in Nonlinear Science and Numerical Simulation* 15: 312-321.

Sezer, S.A. & Yildirim, A. 2010. A numerical treatment for the solution of the hydromagnetic peristaltic flow of a bio-fluid with variable viscosity in a circular cylindrical tube. *International Journal for Numerical Methods in Biomedical Engineering* 26: 1503-1514.

Shafie, S., Mehmood, O.U. & Mustapha, N. 2013. Thermal diffusion and diffusion thermo effects on peristaltic flow of Sisko fluid in non-uniform channel with dissipative heating. *Journal of Heat Transfer, Transactions of ASME* (in press).

Srinivas, S. & Muthuraj, R. 2010. MHD flow with slip effects and temperature dependent heat source in a vertical wavy porous space. *Chemical Engineering Communications* 197: 1387-1403.

Srinivas, S., Gayathri, R. & Kothandapani, M. 2011. Mixed convective heat and mass transfer in an asymmetric channel with peristalsis. *Communications in Nonlinear Science and Numerical Simulation* 16: 1845-1862.

Yildirim, A. & Sezer, S.A. 2010. Effects of partial slip on the peristaltic flow of a MHD Newtonian fluid in an asymmetric channel. *Mathematical and Computer Modelling* 52: 618-625.

Obaid Ullah Mehmood & Sharidan Shafie
Department of Mathematical Sciences
Faculty of Science, Universiti Teknologi Malaysia
81310 Johor Bahru, Johor
Malaysia

Norzieha Mustapha*
UTM Centre for Industrial & Applied Mathematics (UTM-CIAM)
Universiti Teknologi Malaysia
81310 Johor Bahru, Johor
Malaysia

Obaid Ullah Mehmood & T. Hayat
Department of Mathematics
Quaid-I-Azam University 45320
Islamabad 44000
Pakistan

T. Hayat
Department of Mathematics, College of Science
King Saud University, P.O. Box 2455
Riyadh 11451
Saudi Arabia

*Corresponding author; email: norzieha@utm.my